

STUDY OF THE SUITABILITY OF VARIOUS TYPES OF CASTING MATERIALS FOR THE MANUFACTURE OF A SHIP ENGINE

ŠTUDIJA PRIMERNOSTI RAZLIČNIH VRST LITIH MATERIALOV ZA PROIZVODNJO LADIJSKIH MOTORJEV

Juan José Galán^{1*}, Nuria Varela-Fernández¹, Manuel Ángel Graña-López²,
Almudena Filgueira-Vizoso³, Ana García-Diez⁴

¹Department of Naval and Industrial Engineering, ETSI Caminos, Canales y Puertos, University of A Coruña, 15403 Ferrol, Spain

²Department of Industrial Engineering, Escuela Universitaria Politécnica, University of A Coruña, 15405 Ferrol, Spain

³Department of Chemistry, Escuela Politécnica Superior, University of A Coruña, 15403 Ferrol, Spain

⁴Department of Naval and Industrial Engineer, Escuela Politécnica Superior, University of A Coruña, 15403 Ferrol, Spain

Prejem rokopisa – received: 2020-12-28; sprejem za objavo – accepted for publication: 2021-06-15

doi:10.17222/mit.2020.247

The objective of this work was to study the suitability of three types of cast iron for the manufacture of a ship engine: EN-GJS-500-7U for the manufacture of the engine block, EN-GJS-400-15U for the cylinder head and EN-GJL-200 for the liner. Tensile tests were carried out to obtain the ultimate tensile strength (UTS) of each material. The results for the UTS were: 460 MPa for EN-GJS-500-7U, 390 MPa for EN-GJS-400-15U and 170 MPa for EN-GJL-200. Likewise, Brinell-hardness measurements were carried out and the elements present in the materials were determined with spectrometry. Finally, the size of graphite particles in each sample was determined.

Keywords: spheroidal cast iron, grey cast iron, mechanical properties, engine boat

Avtorji v članku opisujejo ustreznost treh vrst sive litine za izdelavo ladijskih motorjev. Litino EN-GJS-500-7U so uporabili za izdelavo bloka motorja, litino EN-GJS-400-15U za glavo cilindra in litino EN-GJL-200 za ohišja ventilov. S pomočjo nateznih preizkusov so bile določene mehanske lastnosti vseh treh litin. Porušna natezna trdnost (UTS) je bila 460 MPa za litino EN-GJS-500-7U, 390 MPa za litino EN-GJS-400-15U in 170 MPa za litino EN-GJL-200. Prav tako je bila določena trdota po Brinellu, s pomočjo spektroskopskih analiz pa še mikrostrukturni elementi in sestava preiskovanih litin. Avtorji so nazadnje opredelili še velikost in obliko grafita v vsakem posameznem vzorcu.

Ključne besede: sferoidno lito železo, siva litina, mehanske lastnosti, ladijski motor

1 INTRODUCTION

Grey cast iron and spheroidal cast iron in particular are used for the manufacture of many engines. This is so because of their wear resistance, appropriate machining property and good castability.¹⁻⁸ In addition, its manufacture is cheaper than that of steel.³ Several papers have been published on its mechanical properties.²⁻¹⁵ Mohebbi et al.¹⁴ studied the fatigue and fracture properties. These authors use the Paris-Erdogan law in order to establish the relationship between the microstructure and fatigue behaviour and fracture toughness of cast iron used in water industry. The study on spheroidal graphite carried out by Hornbogen is more classical.¹⁶ Other studies focus on the macroscopic behavior⁴⁻⁷ in order to correlate microstructure and mechanical behaviour. For example, Collini et al.² measured several specimens of grey cast iron with a pearlitic matrix from different foundries with a servo-hydraulic machine.

As it is well known, the purpose of an engine is to transform any kind of energy into mechanical energy. Its main parts are the engine block, cylinder head and cylinder liner.¹⁷

The engine block of a boat – in our case – is manufactured from cast iron because of its high-temperature strength. In the present work, a spheroidal cast iron, EN-GJS-500-7U, was evaluated in order to establish its suitability for manufacturing the engine block of a cargo ship. Another spheroidal cast iron, EN-GJS-400-15U, was tested to be used for the cylinder head. In the automotive industry, other types of materials, such as Al-Si casting alloys, are being used as alternatives, but not in the case of merchant ships.¹⁷ All the components of an engine block are located inside of it. The main features of this structure are its strength and resistance that support the processes involving high temperatures and pressures occurring inside an engine block. As a block is made of one piece, its production is very complicated. If a block is unsuitable, the process of manufacturing begins again, and the costs and environmental damages increase significantly. Therefore, this research is important as it determines the suitability of a specific material before the start of an engine assembly. Finally, a type of grey cast iron, EN-GJL-200, was evaluated for the production of the cylinder liner. In summary, the goal of this research was to evaluate the suitability of two types of spheroidal graphite cast iron (EN-GJS-500-7U,

*Corresponding author's e-mail:
juan.jose.galan@udc.com (Juan José Galán)

EN-GJS-400-15U) and one type of grey cast iron (EN-GJL-200) for the manufacture of the block, the cylinder head and the cylinder liner of a ship engine. The aim of the manufacturer is that the useful lifetime of the engine is about 30 years.

2 EXPERIMENTAL PART

The manufacturer of the engine block provided samples of EN-GJS-500-7U. A sample was taken from a block of four strokes, 16 cylinders and 7680 kW. The sphericity of graphite as well as the microstructural components of the alloys and the heat treatment have a huge influence on the ductility of cast iron. The fabrication of an engine block requires a large amount of heat. Roughly, it can be outlined in the following way: iron in the liquid state is treated with an additive rich in Mg (between 0.04 w/% and 0.06 w/%) and a silicon alloy is added a few minutes before pouring. The furnace temperature must be above 1450 °C. During the process, two samples are extracted to check the chemical composition. The material is poured into a ladle. When the temperature reaches 1380 °C, the material is cast into a mould. After five days, the casting is extracted from the mould in order to carry out annealing. It is necessary to clean the block with grit blasting.

EN-GJS-500-7U and EN-GJS-400-15U differ during the heat treatment applied. Although annealing heat treatment is applied in both cases, in the first case, the temperature rise rate is 50 °C/h until reaching a maximum temperature of 550 °C, while in the second case, the rate of the temperature rise is 60 °C/h until reaching a maximum temperature of 620 °C. Furthermore, the permanence of the material at 550 °C is 8 h for EN-GJS-500-7U and 10 h for the second case. The cooling rate also varies. In the first case, it is 50 °C/h and in

the second case, it is 30 °C/h. The EN-GJL-200 grey cast iron is different because of a higher percentage of phosphorus. This extra amount of phosphorus gives rise to steadite, Fe₃P, which increases the hardness of the casting. The annealing of this material was similar to the other two cases explained above: a temperature rise at a rate of 30 °C/h up to 550 °C, 6 h of permanence at that temperature, a decrease in the temperature at a rate of 25 °C/h to 100 °C and, finally, cooling down to room temperature. All the tested specimens were obtained from real castings of the engine block, cylinder head and cylinder liner. All the specimens were obtained when the material was removed from the mould, once the heat treatment had been carried out.

Figure 1 shows the equipment used for the tensile test: a tensile testing machine and an extensometer. Equipment calibration was done according to the UNE-EN-7500-1: 2006 standard, using a reference Z4A force transducer.¹⁸ This device can be used in a range between 20 and 500 kN without any loss of accuracy. Table 1 displays the results of the calibration where F_j is the value of the load in kN registered by the tensile testing machine; T1, T2 and T3 are three series of tensile measurements of a sample and the values below them are the values recorded by the reference force transducer; F_a is the mean value of the measurements recorded by the reference force transducer; q is the uncertainty calculated according to Equation (1):

$$q = \frac{(F_j - F_a)}{F_a} \cdot 100 \quad (1)$$

Table 1: Tensile-equipment calibration results

F_j /kN	T1/kN	T2/kN	T3/kN	F_a /kN	q /%
40.00	40.15	40.14	40.13	40.14	-0.30
80.00	80.22	80.15	80.13	80.17	-0.20
160.00	160.24	160.17	160.12	160.18	-0.10
240.00	240.30	240.21	240.13	240.21	-0.10
320.00	320.39	320.29	320.19	320.29	-0.10
400.00	400.52	400.39	400.28	400.39	-0.10



Figure 1: Tensile testing machine and extensometer

The specimens for the tensile test of the cylinder liner were manufactured in accordance with the UNE-EN 1561: 2012¹⁹ standard, while the ones for the cylinder head and the block, UNE-EN 1563: 2012²⁰ was used. The tensile test was carried out according to UNE-EN 10002-1: 2015.²¹

The Brinell hardness test was carried out according to the UNE-EN ISO 6506-1: 2015²² and UNE-EN ISO 6506-2: 2015 standards.²³ To measure the Brinell hardness, a Hoytom model 1003-A durometer was used. The test was carried out with a load of 1839 N and a 2.5 mm diameter tungsten carbide ball indenter.

The chemical composition of the specimens was determined with a S4 Pioneer Bruker X-ray fluorescence spectrometer. Also, to determine the carbon and sulphur contents, a carbon analyser (LECO C-200) was used.

In addition to these techniques, a metallographic analysis was also performed. To do this, a part of the tensile test sample was taken from the head of the tensile specimen and its surface was polished. Next, the polished sample was filled with a phenolytic resin and polished again. Subsequently, the encapsulated and polished sample was subjected to a chemical attack with 2 % Nital for 2 min. After etching, the sample was washed with cold water and, finally, with alcohol. Its observation was carried out with a microscope of 100× and 400× magnifications, OLYMPUS model BH2.

3 RESULTS AND DISCUSSION

3.1 Engine block

The specimen used in the test – spheroidal cast iron EN-GJS-500-7U – was prepared according to the specifications given in the UNE-EN 1563: 2012 standard. It had a circular section and its area was 153.50 mm²; its initial length $L_0 = 70$ mm and its total length was 100 mm. **Figure 2** shows the typical stress-strain curve obtained during the tensile test. The experiment was carried out with a speed of the upper body of the tensile testing machine of 1.1 kN/s. The upper body of the machine carries the force, while the lower body remains static to maintain the position of the sample.

According to these results, carried out at room temperature, the material did not show any brittle fracture although its plastic behaviour was not very remarkable. As many researchers pointed out, high cooling rates affect the dendritic network and the eutectic-cell structure, resulting in good mechanical properties; however, if the amount of carbon increases, the mechanical properties are affected negatively.^{24–31}

The ultimate tensile strength during this test was about 460 MPa and its elongation was around 12 %. These results comply with the specifications given in the UNE-EN-1563: 2012 standard, which prescribes, for a sample of a 3-mm or 4-mm wall thickness, a minimum tensile strength of 450 MPa and a minimum elongation of 7 %.

Hardness needed to be measured to understand the machinability of the material. Brinell hardness was measured according to UNE-EN 1563: 2012; the hardness of a material must be between 100 HB and 230 HB in order to be suitable for an engine block. The Brinell hardness

obtained in this work was 201 HB. Hafiz²⁸ experimentally estimated the relationship between the Brinell hardness and pearlite contents in a spheroidal-graphite iron casting. This relationship is shown in Equation (2):

$$HB = 0.0128P^2 + 0.1865P + 127.78 \quad (2)$$

where HB is the Brinell hardness and P represents the percentage of pearlite. In our case, the specimen had approximately 70 % of pearlite. According to Equation (2), Brinell hardness increases abruptly with the amount of pearlite in the material. This is because the hardness of pearlite is affected by the cooling of the casting after the solidification.²⁹ The results for the mechanical properties are summarized in **Table 2**.

Table 2: Mechanical properties of the EN-GJS-500-7 U sample from the engine block

Property	Value
Elongation (ΔL)	8.40 mm
Ultimate yield strength (σ_s)	460 MPa
Percentage of elongation	12 %
0.2 % offset yield strength ($\sigma_{0.2}$)	437 MPa
Brinell hardness	201 HB

The sample was chemically analysed with spectrometry in order to identify the amounts and types of elements present in the material. **Table 3** depicts the percentage by weight of each element present in the analysed sample. The composition of this sample is in accordance with the average composition of this kind of iron castings.³²

Table 3: Chemical analysis of the EN-GJS-500-7 U sample from the engine block

Element	w/%
Carbon	3.62
Silicon	2.49
Manganese	0.29
Phosphorus	0.018
Sulphur	0.015
Titanium	0.009
Magnesium	0.040
Copper	0.44

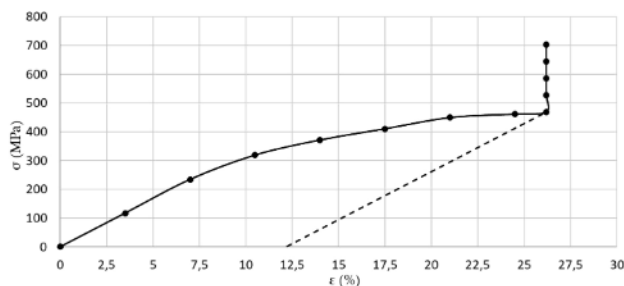


Figure 2: Stress-strain curve for an EN-GJS-500-7 U sample from the engine block

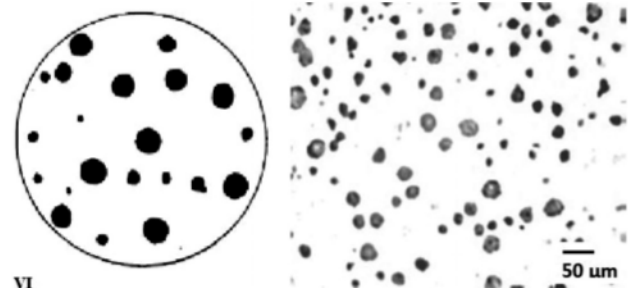


Figure 3: Model given by the UNE-EN 945-1: 2012 standard and a material sample at a magnification of 100×

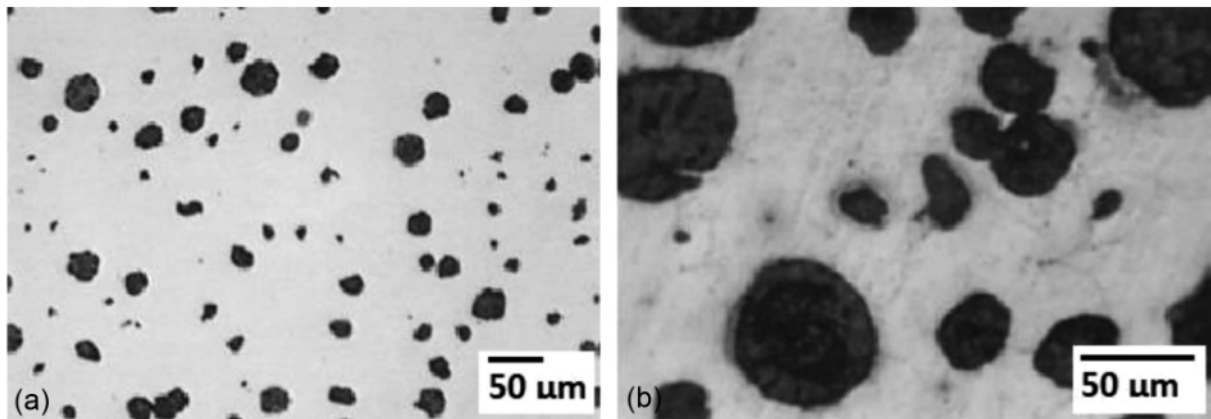


Figure 4: Sample of EN-GJS-400-15U at magnifications: a) 100×, b) 400×

In order to determine the shape and size of graphite particles, UNE-EN 945-1: 2012³³ was used. Methodology by comparison was used. In the present case, the size of the graphite particles was between 0.015 mm and 0.039 mm. A real sample at a magnification of 100× and a model are shown in **Figure 3**.

3.2. Cylinder head

Spheroidal cast iron EN-GJS-400-15 U was used for the cylinder head. The UNE-EN-1563: 2012 standard determines for this material – a sample with a 3-mm or 4-mm wall thickness – that the tensile strength must be at least 390 MPa and the minimum elongation must be 15 %. The results obtained with the mechanical tests are shown in **Table 4** and the chemical composition in percentage by weight is in **Table 5**.

Table 4: Mechanical properties of the EN-GJS-400-15 U sample from the cylinder head

Property	Value
Elongation (ΔL)	11.2 mm
Ultimate yield strength (σ_s)	469 MPa
Percentage of elongation	16 %
0.2 % offset yield strength ($\sigma_{0.2}$)	301 MPa
Brinell hardness	172 HB

Table 5: Chemical analysis of the EN-GJS-400-15 U sample from the cylinder head

Element	w/%
Carbon	3.63
Silicon	2.21
Manganese	0.18
Phosphorus	0.016
Sulphur	0.021
Magnesium	0.051
Copper	0.096

Figure 4 shows a sample of the material. The procedure was the same as in the previous case, the image taken at the 100× magnification was compared with that from UNE-EN-945-1: 2012. From this comparison, it

was determined that the graphite is 90 % spheroidal and that its shape corresponds to type VI from the standard. To determine the size, the same standard was used. It gives the guideline for the size of the particles. In the present case, the size was between 0.03 mm and 0.06 mm.

3.3. Cylinder liner

As in the previous cases, a tensile test, a hardness test, a chemical analysis and a metallographic analysis were carried out for the study and characterization of the cylinder-liner sample. In this case, the material used was grey cast iron, EN-GJL-200. The UNE-EN 1561: 2012 standard establishes a minimum tensile strength of 170 MPa for this type of material. The sample was made in accordance with this standard; the length of the specimen was 96 mm and its cross-section area was 824 mm². As can be seen in **Figure 5**, the tensile strength was around 300 MPa, thus complying with the requirements of the standard.

Here, a brittle fracture can be seen on the sample. Hardness tests for this material showed a hardness of 240 HB. The hardness of this sample was 19 % greater than that of the engine block and almost 40 % greater than that of the cylinder head. Brittle fracture is of utmost importance for the cylinder liner as it prevents damage to the engine block in the event of its breakage.

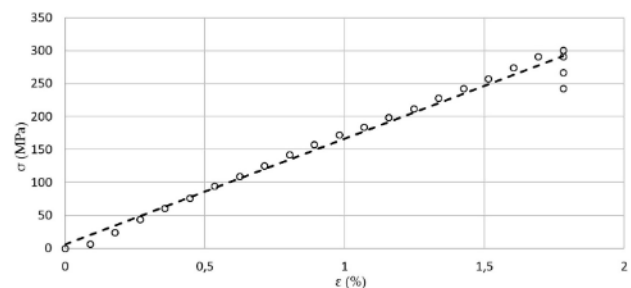


Figure 5: Stress-strain curve for the EN-GJL-200 sample from the cylinder liner

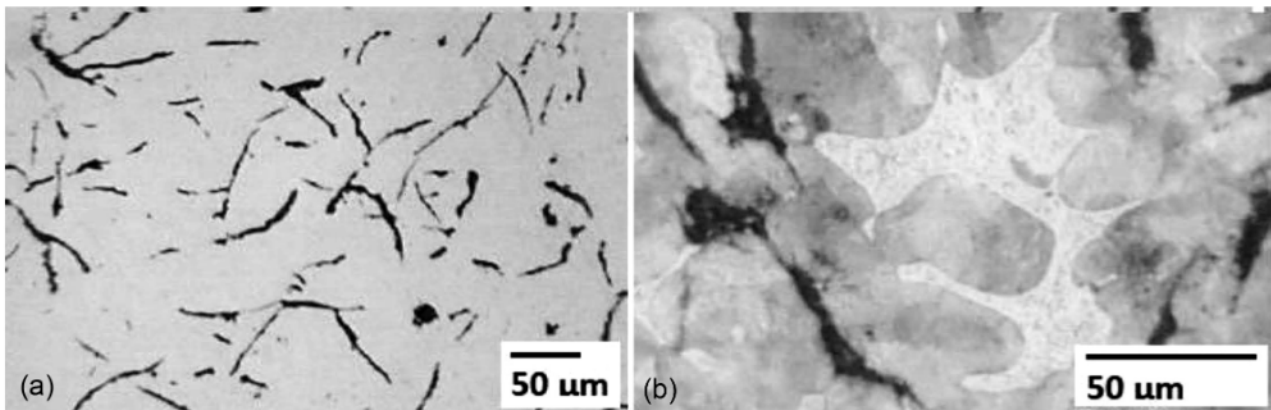


Figure 6: a) Sample of EN-GJL-200 at the magnification of 100×, b) sample of EN-GJL-200 at the magnification of 400×

The chemical composition of the cylinder-liner sample can be seen in Table 6.

Table 6: Chemical analysis of the EN-GJL-200 sample from the cylinder liner

Element	w/%
Carbon	3.02
Silicon	1.32
Manganese	0.80
Phosphorus	0.44
Sulphur	0.025
Titanium	0.38
Vanadium	0.24

The fragility of the material is a result of a high percentage of phosphorus, 0.44 w/%, in this sample. In the two previous cases studied, the percentage of phosphorus was 0.016 w/% and 0.018 w/%, respectively. Furthermore, in this type of cast iron, the stresses tend to concentrate at the ends of laminar graphite. This is also a reason for a lower ultimate tensile strength and fragile fracture.

Figure 6a shows the laminar shape of graphite and the pearlitic structure with steadite. The image was taken at the 100× magnification. In Figure 6b, taken at the 400× magnification, the pearlite and steadite (the white part) can be seen in greater detail.

The size of the graphite particles in this sample (UNE-945-1: 2012 standard) is between 0.12 mm and 0.25 mm.

4 CONCLUSIONS

In the present work, an analysis of three types of cast iron is reported: two spheroidal types (EN-GJS-500-7U and EN-GJS-400-15U) and one example of grey cast iron (EN-GJL-200) intended for the manufacture of three important components including an engine block, a cylinder head and a cylinder liner were analysed. All the tested samples comply with the corresponding standards; the main conclusions are detailed below.

The values obtained for the ultimate tensile strength of the alloys studied are as follows: 460 MPa for EN-GJS-500-7U; 390 MPa for EN-GJS-400-15U; and 170 MPa for EN-GJL-200.

The hardness of grey cast iron was by about 19 % higher than that of EN-GJS-500-7U and by 40 % higher than that of EN-GJS-400-15U. The matrix of the EN-GJL-200 sample is made up of pearlite and steadite, while the spheroidal cast iron samples are made up of ferrite and pearlite. This explains the brittle behaviour of the EN-GJL-200 alloy.

Acknowledgment

This article is derived from the doctoral thesis of Nuria Varela Fernández.

5 REFERENCES

- ¹ M. W. Shin, G. H. Jang, J. H. Kim, H. Y. Kim, H. Jang, The Effect of Residual Stress on the Distortion of Grey Iron Brake Disks, *J. Mater. Eng. Perform.*, 22 (2013), 1129–1135, doi:10.1007/s11665-012-0397-7
- ² L. Collini, G. Nicoletto, R. Konecna, Microstructure and Mechanical Properties of Pearlitic Grey Cast Iron, *Mater. Sci. Eng. A*, 488 (2008) 1–2, 529–539, doi:10.1016/j.msea.2007.11.070
- ³ M. N. James, L. Wenfong, Fatigue Crack Growth in Austempered Ductile and Grey Cast Irons – Stress Ratio Effects in Air and Mine Water, *Mater. Sci. Eng. A*, 265 (1999) 1–2, 129–139, doi:10.1016/S0921-5093(98)01140-X
- ⁴ M. Moonesan, F. Madah, Effect of alloying elements on thermal shock resistance of grey cast iron, *J. Alloys Comp.*, 520 (2012), 226–231, doi:10.1016/j.jallcom.2012.01.027
- ⁵ F. Zieher, F. Langmayr, A. Jelatancev, K. Wieser, Thermal mechanical fatigue simulation of cast iron cylinder heads, *SAE Technical Papers*, 2005, doi:10.4271/2005-01-0796
- ⁶ T. J. Mackin, K. Noe, S. C. Ball, B. Bedell, D. Bim-Merle, M. Bingaman, D. Bomleny, G. Chemlir, D. Clayton, H. Evans, Thermal cracking in disc brakes, *Eng. Fail. Anal.*, 9 (2002) 1, 63–76, doi:10.1016/S1350-6307(00)00037-6
- ⁷ D. Taylor, J. Li, A. Giese, Short Fatigue Crack Growth in Cast Iron Described Using P-A Curves, *Int. J. Fatigue*, 17 (1995) 3, 201–206, doi:10.1016/0142-1123(95)98940-5

- ⁸ D. Taylor, M. Hughest, D. Allen, Notch Fatigue Behaviour in Cast Irons Explained Using a Fracture Mechanics Approach, *Int. J. Fatigue*, 18 (1996) 7, 439–445, doi:10.1016/0142-1123(96)00018-7
- ⁹ A. N. Damir, A. Elkhatab, G. Nassef, Prediction of Fatigue Life Using Modal Analysis for Grey and Ductile Cast Iron, *Int. J. Fatigue*, 29 (2007) 3, 499–507, doi:10.1016/j.ijfatigue.2006.05.004
- ¹⁰ P. Baicchi, L. Collini, E. Riva, A Methodology for the Fatigue Design of Notched Castings in Grey Cast Iron, *Eng. Fract. Mech.*, 74 (2007) 4, 539–548, doi:10.1016/j.engfracmech.2006.04.018
- ¹¹ D. D. Goettsch, J. A. Dantzig, Modeling Microstructure Development in Grey Cast Irons, *Metall. Mater. Trans. A*, 25 (1994), 1063–1079, doi:10.1007/BF02652281
- ¹² D. J. Weinacht, D. F. Socie, Fatigue Damage Accumulation in Grey Cast Iron, *Int. J. Fatigue*, 9 (1987) 2, 79–86, doi:10.1016/0142-1123(87)90048-X
- ¹³ S. H. Choo, S. Lee, S. J. Kwon, Surface Hardening of a Grey Cast Iron Used for a Diesel Engine Cylinder Block Using High-Energy Electron Beam Irradiation, *Metall. Mater. Trans. A*, 30 (1999), 1211–1221, doi:10.1007/s11661-999-0271-x
- ¹⁴ H. Mohebbi, D. A. Jesson, M. J. Mulheron, P. A. Smith, The Fracture and Fatigue Properties of Cast Irons Used for Trunk Mains in the Water Industry, *Mater. Sci. Eng. A*, 527 (2010) 21–22, 5915–5923, doi:10.1016/j.msea.2010.05.071
- ¹⁵ J. H. Bulloch, Near Threshold Fatigue Behaviour of Flake Graphite Cast Irons Microstructures, *Theor. Appl. Fract. Mech.*, 24 (1995) 1, 65–78, doi:10.1016/0167-8442(95)00032-A
- ¹⁶ E. Hornbogen, Fracture toughness and fatigue crack growth of grey cast irons, *Journal of Materials Science*, 20 (1985), 3897–3905, doi:10.1007/BF00552378
- ¹⁷ M. Javidiani, D. Larouche, Application of cast Al-Si alloys in internal combustion components, *Int. Mater. Rev.*, 59 (2014) 3, 132–158, doi:10.1179/1743280413Y.0000000027
- ¹⁸ UNE-EN-ISO 7500:2006. Metallic materials – Verification of static uniaxial testing machines – Part 1: Tension/compression testing machines – Verification and calibration of the force-measuring system (ISO 7500-1:2004)
- ¹⁹ UNE-EN 1561:2012. Founding – Grey cast irons
- ²⁰ UNE-EN 1563:2012. Spheroidal graphite cast irons
- ²¹ UNE-EN 10002-1: 2015. Metallic materials – Tensile testing – Part 1: Method of test at ambient temperature
- ²² UNE-EN ISO 6506-1: 2015. Metallic materials – Brinell hardness test – Part 1: Test method (ISO 6506-1:2014)
- ²³ UNE-EN ISO 6506-2: 2015. Metallic materials – Brinell hardness test – Part 2: Verification and calibration of testing machines (ISO 6506-2:2014)
- ²⁴ M. Hafiz, Mechanical properties of SG-iron with different matrix structure, *Journal of Materials Science*, 36 (2001), 1293–1300, doi:10.1023/A:1004866817049
- ²⁵ H. T. Angus, Cast Iron Physical and Engineering Properties, Butterworths, London, Boston 1976
- ²⁶ G. F. Ruff, J. F. Wallace, Effects of solidification structures on the tensile properties of grey iron, *AFS Trans.*, 56B (1977), 179–202
- ²⁷ C. Bates, Alloy element effect on lamellar iron properties: part II, *AFS Trans.*, 94 (1986), 889–905
- ²⁸ O. Liesenberg, J. Ohser, Die beziehung zwischen der zugfestigkeit und der graphitusbildung von gusseisen mit lamellengraphit, *Giessereitechnik*, 29 (1983), 106–108
- ²⁹ H. Nakae, H. Shin, Effect of graphite morphology on tensile properties of flake graphite cast iron, *Mater. Trans.*, 42 (2001) 7, 1428–1434, doi:10.2320/matertrans.42.1428
- ³⁰ T. H. Willidal, W. Bauer, P. Schumacher, Stress/strain behavior and fatigue limit of grey cast iron, *Mater. Sci. Eng. A*, 413–414 (2005), 578–582, doi:10.1016/j.msea.2005.08.200
- ³¹ V. Fourlakidis, L. V. Diaconu, A. Diószegi, Effects of Carbon Content on the Ultimate Tensile Strength in Lamellar Cast Iron, Solidification and Gravity V, *Mater. Sci. Forum*, 649 (2010), 511–516, doi:10.4028/www.scientific.net/MSF.649.511
- ³² T. J. Baker, The fracture resistance of the flake graphite cast iron, *Mater. Eng. Appl.*, 1 (1978) 1, 13–18, doi:10.1016/0141-5530(78)90003-1
- ³³ UNE-EN 945-1:2012. Microstructure of cast irons – Part 1: Graphite classification by visual analysis (ISO 945-1:2008)